fiducial reference measurements for satellite ocean colour

Technical Report TR-5 “Protocols and Procedures to Verify the Performance of Fiducial Reference Measurement (FRM) Field Ocean Colour Radiometers (OCR) used for Satellite Validation

Title	Technical Report TR-5 “Protocols and Procedures to Verify the Performance of Fiducial Reference Measurement (FRM) Field Ocean Colour Radiometers (OCR) used for Satellite Validation
Document reference	FRM4SOC-TR5
Project	ESA – FRM4SOC
Contract	ESRIN/Contract No. 4000117454/16/1-SBo
Deliverable	D-130 (Technical Report TR-5)
ATTN	Craig Donlon ESA/ESTEC Technical Officer Keplerlaan 1 2201 AZ Noordwijk The Netherlands
Version	**DRAFT 1.1**
Date issued	07.12.2016

	Prepared by	**Signed By**	**Approved by**
Name:	Joel Kuusk	Riho Vendt	Craig Donlon
Organisation:	Tartu Observatory	Tartu Observatory	ESA/ESTEC
Position:	WP leader	Project manager	Technical Officer
Date:			
Signature:			

Fiducial Reference Measurements for Satellite Ocean Colour (FRM4SOC) – Laboratory Calibration Exercise 2 (LCE-2): Verification of Fiducial Reference Measurement Ocean Colour Radiometers (FRM OCR)

D-130: Protocols and Procedures to Verify the Performance of Fiducial Reference Measurement (FRM) Field Ocean Colour Radiometers (OCR) used for Satellite Validation (TR-5)

TECHNICAL REPORT

Joel Kuusk, Ilmar Ansko, Viktor Vabson, Martin Ligi, Riho Vendt

Document Control Table

Title	Technical Report TR-5 "Protocols and Procedures to Verify the Performance of Fiducial Reference Measurement (FRM) Field Ocean Colour Radiometers (OCR) used for Satellite Validation
Document reference	FRM4SOC-TR5
Project	ESA – FRM4SOC
Contract	ESRIN/Contract No. 4000117454/16/1-SBo
Deliverable	D-130 Technical Report TR-5
Version	**DRAFT 1.1**
Date Issued	07.12.2016

Document Change Record

Index	Issue	Revision	Date	Brief description	Issued by
0.	1	0	31.08.2016	DRAFT	Riho Vendt
1.	1	1	07.12.2016	Updated schedule	Joel Kuusk

Distribution List

Company/Organisation	Name	Format	No. of Copies
TO	Riho Vendt	Electronic file	1
TO	Viktor Vabson	Electronic file	1
TO	Joel Kuusk	Electronic file	1
TO	Anu Reinart	Electronic file	1
TO	Ilmar Ansko	Electronic file	1
TO	Martin Ligi	Electronic file	1

Contents

Executive Summary

This information will be provided in the final version of this document.

Acronyms and Abbreviations

Acronym	Abbreviation
AAOT	Aqua Alta Oceanographic Tower
ADC	Analog-to-digital converter
AERONET	Aerosol Robotic Network
CDOM	Colored dissolved organic matter
EO	Earth Observation
ESA	European Space Agency
EUMETSAT	European Organisation for the Exploitation of Meteorological Satellites
FICE	Field Inter-Comparison Experiment
FOV	Field of View
FRM4SOC	Fiducial Reference Measurements for Satellite Ocean Colour
IOP	Inherent Optical Properties
ISO	International Organization for Standardization
LCE	Laboratory Comparison Experiment
LSF	Line Spread Function
MSI	MultiSpectral Instrument
MVSM	Multi-spectral Volume Scattering Meter
MVT	Meris Validation Team
NPL	National Physical Laboratory
OC	Ocean Colour
OLCI	Ocean and Land Colour Instrument
PAR	Photosynthetically active radiation
QTH	Quartz Tungsten Halogen
SI	Systeme International d'Unites
SLM	Stray Light Correction Matrix
SSF	Slit-Scattering Function
TO	Tartu Observatory
TR	Technical Report
TSM	Total Suspended Matter

UTC	Coordinated Universal Time
VSF	Volume Scattering Function

List of symbols

Symbol	Definition
E	Irradiance
E_d	Downwelling irradiance
G_C	Gain amplification factor
λ	Wavelength
L	Radiance
L_d	Downwelling radiance
L_u	Upwelling radiance
L_w	Water-leaving radiance
n	Refractive index of water
R_E	Irradiance responsivity
R_{RS}	Remote sensing reflectance
τ_a	Aerosol optical thickness
θ_s	Solar zenith angle
θ_v	View zenith angle
w_s	Wind speed

1 Scope

The core action of the FRM4SOC project is to ensure that ground-based measurements of ocean colour parameters are traceable to SI standards in support of ensuring high quality and accurate Sentinel-2 MSI and Sentinel-3 OLCI products. The FRM4SOC project contributes directly to the work of ESA and EUMETSAT to ensure Sentinel-3 OLCI and Sentinel-2 MSI instruments are validated in orbit.

LCE-2 links the OC field measurements to the SI-traceable calibration and verifies whether different instruments measuring the same object can provide consistent results within the uncertainty limits.

Involvement of all relevant expertise available in Europe and worldwide is in line with the objectives of the project and in the interest of the EO/ocean colour community. Therefore, it is anticipated that all interested parties in this wider community, but outside the Consortium, should be able to participate in the comparison exercise as external participants. Tartu Observatory (TO) will publish a global open invitation for LCE-2 to involve as many active users of Field Ocean Colour Radiometers as possible. Information about participating instruments will be gathered and TO will work together with the participants in order to make sure that all the necessary soft- and hardware for mounting the instruments in the lab and during the outdoor intercomparison will be available for the time of LCE-2. The OC radiometers participating in the exercise will be gathered to TO prior LCE-2 for absolute radiometric calibration. Participants will join afterwards for comparison measurements. TO will help the participants with all aspects concerning travel, accommodation, customs, shipping of instruments, etc.

2 Introduction

The LCE-2 will serve as a preparation stage for the AAOT-FICE field intercomparison exercise. The LCE-2 can be divided into three sub-tasks:

1) Provide SI-traceable radiometric calibration for participating radiometers
2) Organize indoor intercomparison in controlled environment
3) Organize outdoor intercomparison over terrestrial water surface

It is not feasible to calibrate all parameters (wavelength accuracy, stray light, field of view, temperature stability, linearity, angular response for irradiance sensors, etc.) of all the participating instruments during LCE-2. However, all participants of LCE-2 are encouraged to have their instruments as well characterised as possible prior to LCE-2. Absolute radiometric calibration will be performed for all the participating radiometers just before the LCE-2.

LCE-2 will take place before AAOT-FICE on 08.05.2017 – 13.05.2017. It will serve as a training session for the participants of AAOT-FICE as well as provide SI-traceable radiometric calibration of participating radiometers. Previous inter-comparison of ocean colour radiometers has shown that the consistency of results improved when all the instruments participating in the inter-calibration were radiometrically calibrated in the same laboratory [1].

TO will serve as the main organizer for this comparison, supported by NPL. TO will be responsible for inviting participants and for the analysis of data, following appropriate processing by individual participants. TO will be the only organisation to have access and to view all data from all the participants. This data will remain confidential to the participant and TO at all times, until the publication of the report showing results of the comparison to participants.

3 Organisation of the Comparison

The event is organised by Tartu Observatory, a public research and development authority, administered by the Estonian Ministry of Education and Research operating under the Research and Development Act, other laws and international contracts.

3.1 Participation guidelines

By their declared intention to participate in this key comparison, the participants accept the general instructions and the technical protocols written down in this document and commit themselves to follow the procedures strictly.

Registration will be opened from 01.11.2016 to 20.12.2016. Registration will be made through online form on the project's website, which will follow the structure seen in appendices 1 and 2 of the LCE-2 implementation plan. During the registration, the participants have to fill in the description about the radiometers they are bringing to the event. As the site for field measurements is with limited size, only one set of radiometers is allowed per participating institute. The acceptance/rejection on the participation will be sent to all applicants in the beginning of January 2017.

3.2 Participants

As the maximum number of participants to be handled is 15, then the participants for LCE-2 will be selected by the following criteria in the following order:

1) Partnership in FRM4SOC
2) Participation in FICE
3) Participation in LCE-1
4) Fully characterised radiometers of the participant
5) For the rest, first come, first served

3.3 Form of Comparison

This information will be provided in the final version of this document.

3.4 Schedule

The following schedule is planned for LCE-2.

1) Registration opened: 01.11.2016 – 20.12.2016
2) Confirmed list of participants: beginning of January 2017
3) Arrival of the participating instruments to TO: 24.04.2017
4) Main activities of LCE-2: 08.05.2017 – 13.05.2017.

More details of the Agenda are available in the Implementation Plan for LCE-2 (LCE-2-IP).

4 Facilities

4.1 Radiometric calibration

The radiometric calibration and indoor intercomparison will take place at Tartu Observatory, located in Tõravere, Estonia. TO has modern, well equipped facilities for research work, an excellent visitor centre, and new laboratory complex. In 2012, a new laboratory complex at the premises of TO has been established for development and testing of new technologies including stations for development, prototyping, and assembly; facilities for climatic, thermal-vacuum, vibration, and electromagnetic compatibility (EMC) testing; workshops for mechanical construction and repair works of scientific instruments. The laboratories have independent and automatic control for temperature and humidity. Special conditions as electrostatic discharge protected environment (ESD), anechoic chamber, and cleanrooms (EN ISO 14644 Class 8) have been established. Three rooms in cleanroom environment with total area of 100 m² are available for optical measurements. Optical laboratory includes passive damping setup tables, one of them on separately built foundation for vibration-free measurements.

The key elements of the existing laboratory equipment for establishment of the spectral irradiance scale include: FEL lamps, 1000 W with spectral irradiance calibrated in the wavelength range of (250…2500) nm and relative uncertainty 1.2%…8% depending on wavelength; filter radiometer based on three-element Si trap detector for the spectral range of (340…950) nm; filter radiometer based on three-element InGaAs trap detector for the spectral range of (900…1550) nm; diffuse reflectance targets with diameter of (10…30) cm, and calibrated reflectance factor of 2%…99%; 450 W stabilized Xe arc source (Newport/Oriel); radiometric power supplies for calibration lamps; scanning monochromators, including double LOMO SDL-1 with spectral range of (200…6000) nm, and Bentham DTMS300 with spectral range of (200…2500) nm, fully automated for spectral measurements; linear and rotary translation stages; stabilized He-Ne laser (633 nm, output power of 1.5 mW, long-term stability 0.2%, from Thorlabs); electrically calibrated pyroelectric radiometer RS-5900 in the spectral range of (250…3000) nm, input power 5 µW…100 mW, with relative uncertainty of 1%; Integrating spheres with diameters from 5 cm to 1.2 m; calibrated power supplies and measurement electronics, photomultiplier detectors, environmental testing boxes, optical shutters, mounting tables, rubidium based high precision reference frequency source with the long term frequency stability of 10^{-12}.

In order to assure and demonstrate the reliability of the calibration services, the quality management procedures are being developed and applied. For establishment of the metrological traceability of measurement results the reference instruments are calibrated at National Metrology Institutes or accredited calibration laboratories (NPL, UK; MRI-MIKES, Finland; Metrosert, Estonia). The stability of the reference standards and measurement instruments is regularly monitored in the intermediate period of subsequent calibrations.

Regular calibration and characterisation of several common types of radiometers used for OCR (e.g. TriOS RAMSES, Satlantic TACCS, Water Insight WISP-3) is performed at the laboratories of TO. A special study for characterisation of the OCR radiometers for quantification of the effect of stray light and the possible methods for its correction is in progress [2], [3].

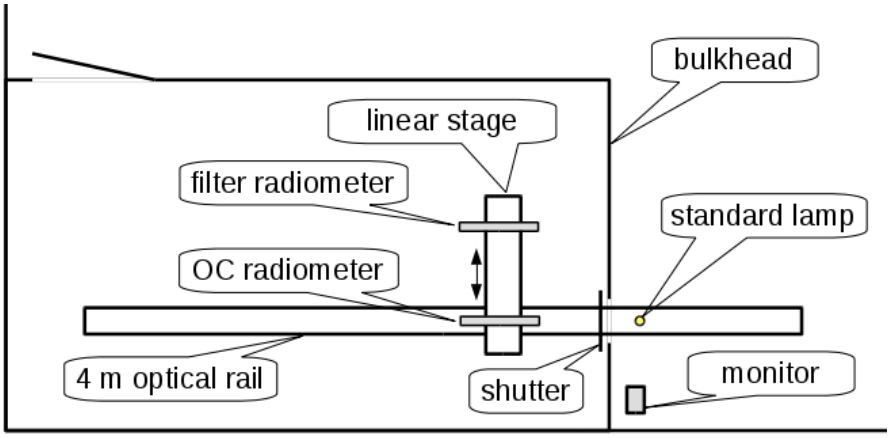

Figure 1: Irradiance sensor calibration setup of TO.

4.1.1 Calibration of irradiance sensors

Link to the international SI scale is provided via an FEL lamp calibrated at NPL during LCE-1. The lamp is powered by a stabilized radiometric power supply Newport/Oriel 69935. The lamp is operated in constant current mode. A custom designed circuit is used for monitoring the lamp current through a 10 mΩ shunt resistor P310 and providing feedback to the power supply. Lamp current is stabilized to better than 1 mA. The same feedback unit is used for logging the lamp current and voltage. Voltage is measured with a 4-wire sensing method from the connector of the lamp socket. The lamp and OC radiometer being calibrated are mounted on an optical rail that passes through a bulkhead which separates the lamp and radiometer during calibration (Figure 1). A computer-controlled electronic shutter Melles Griot 04UTS268 with a ∅64 mm aperture is attached to the bulkhead. The shutter is used for dark signal measurements during calibration. Two additional baffles with ∅60 mm apertures are placed between the bulkhead and the radiometer at 50 mm and 100 mm distances from the bulkhead. The OC radiometer being calibrated is mounted next to a filter radiometer on a computer-controlled linear translation stage which allows perpendicular movement with respect to the optical rail. The positions of both radiometers are carefully adjusted before calibration and the translation stage positions saved in the controlling software. This allows fast and accurate swapping of the radiometers when the lamp is turned on. The filter radiometer is used for monitoring possible long term drifts of the standard lamp. The filter radiometer is based on a 3-element trap detector with Hamamatsu S1337-11 windowless Si photodiodes and temperature-controlled bandpass filters with peak transmittances at nominal wavelengths 340 nm, 350 nm, 360 nm, 380 nm, 400 nm, 450 nm, 500 nm, 550 nm, 600 nm, 710 nm, 800 nm, 840 nm, 900 nm, 950 nm, and 980 nm. The photocurrent of the filter radiometer is amplified and digitized with a Bentham 487 current amplifier with integrating ADC. Newport 350B temperature controller is used for stabilizing the temperature of the bandpass filters. The filters are changed manually and it takes about two minutes for the temperature of the filter to stabilize. As the OC radiometer and filter radiometer cannot be used simultaneously, an additional broadband monitor sensor is used for recording short time changes in the lamp intensity during calibration. The monitor is a single S1337BQ-1010 photodiode connected to a proprietary datalogger. The distance between the lamp and the radiometer is measured with a custom designed measurement probe. One end of the probe is placed against the socket of the lamp and the other end of the probe has two lasers with intersecting beams. The point of intersection defines the other endpoint of the probe. Such a design allows contactless distance measurement and there is no need for touching the diffuser surface of the radiometer. The contactless probe is especially handy if the diffuser is covered with a protective glass dome. The measurement precision of the distance probe is 0.1 mm.

4.1.2 Calibration of radiance sensors

Radiance sensor calibration setup (Figure 2) is based on the lamp/plaque method and utilizes the same components as the irradiance sensor calibration setup. A Sphere Optics sg3151 (200×200) mm calibrated white reflectance standard is mounted on the linear translation stage next to the filter radiometer. Normal incidence for the illumination and 45° from normal for viewing are used. The panel

is calibrated in the same illumination and viewing conditions at NPL during LCE-1. A mirror in a special holder and an alignment laser are used for aligning the plaque and radiance sensor.

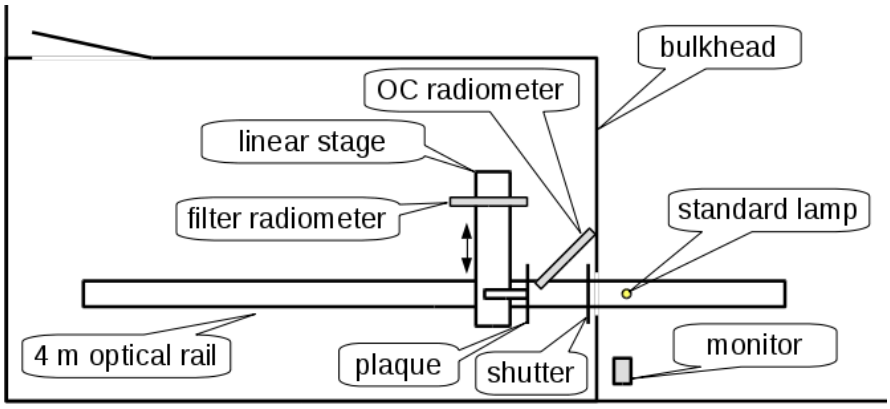

Figure 2: Radiance sensor calibration setup of TO.

4.2 Indoor intercomparison

The indoor intercomparison will take place at Tartu Observatory, Estonia. Stable radiance and irradiance sources are used for verifying the performance of OC radiometers.

4.2.1 Intercomparison of irradiance sensors

An FEL lamp is used as a stable irradiance source for indoor intercomparison. The power supply, feedback unit, monitor detector, and distance measurement probe are the same as used for the radiometric calibration, but the FEL lamp will be different.

4.2.2 Intercomparison of radiance sensors

A Bentham ULS-300 integrating sphere with internal illumination (Figure 3) is used as a stable radiance source. ULS-300 is a ∅300 mm integrating sphere with ∅100 mm target port. According to the manufacturer the uniformity of radiance over the output aperture is ±0.05% independent of the intensity setting. The sphere has a single 250 W quartz tungsten halogen light source and an 8-branch fibre for transporting the light into the sphere. The intensity of light inside the sphere can be changed with a variable mechanical slit placed between the light source and the fibre bundle. This design allows changing the intensity while maintaining the spectral composition of light which corresponds to correlated colour temperature (3100±20) K. The lamp is powered by a Bentham 605 stabilized power supply. A Gigahertz-Optik VL-3701-1 broadband illuminance sensor attached directly to the sphere is used as monitor detector. The monitor current is recorded by a proprietary datalogger.

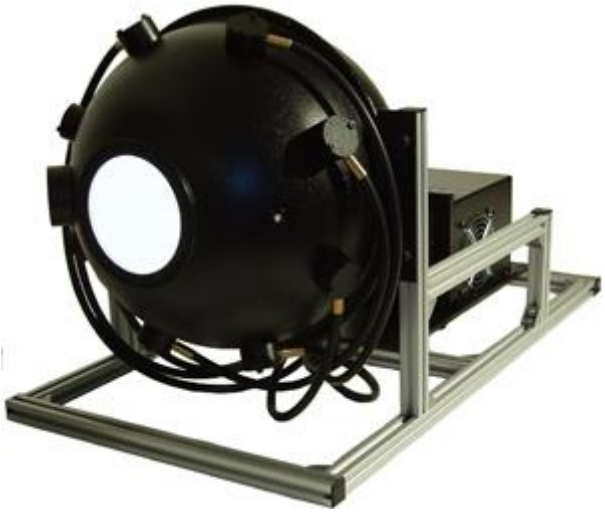

Figure 3: Bentham ULS-300 integrating sphere.

4.3 Outdoor intercomparison

The outdoor intercomparison will take place at Lake Kääriku, Estonia, 58° 0' 5" N, 26° 23' 55" E (Figure 4). Kääriku is a small village located in south eastern Estonia, 30 km south of Tõravere (approximately 45 minutes' drive by car).

Lake Kääriku is a eutrophic lake. It has an irregular shape with the surface area of 19.8 ha (length 650 m, width 550 m). It has rather small catchment area (4.8 km^2). Maximum depth is 5.9 m, with an average of 2.6 m. The water colour is greenish-yellow, measured transparency (Secchi disk depth) is 1.8 m. The average chlorophyll content Chl = 11.9 mg m^{-3}, total suspended matter content is TSM = 3.5 g m^{-3}, diffuse attenuation coefficient of downwelling irradiance K_d(PAR) = 1.3 m^{-1}. The bottom is muddy. The lake has only a weak inflow, water exchanges twice a year. According to EU Water Framework Directive, it is unstratified lake with medium alkalinity (type II). It is classified as macrophyte-dominated shallow lake. Macrophytic vegetation is dominated by helophytes.

Lake Kääriku has a 50 m long pier and a diving platform on the southern coast (Figures 4 and 5). The diving platform has two levels. The upper level is 5.7 m above the water surface and the handrail of the upper level is 6.8 m above the water surface (

Figure 6). Depth of water around the diving platform is 2.6 m to 3.6 m (Figure 7). Depth was measured with a Plastimo Echotest 2 handheld depth sounder. Closest trees are about 65 m south of the platform, the treetops are less than 20° above the horizon when viewed from the upper level of the platform. The modelled shadows of the tower around noon and two hours before noon in the middle of May can be seen in Figure 8. The cones in Figure 8 represent the 7° field-of-view (FOV) of a TriOS RAMSES spectroradiometer in the typical view configuration of 40° nadir angle and 135° relative azimuth angle from the principal plane.

Figure 4: Lake Kääriku.

Figure 5: Pier and diving platform of Lake Kääriku.

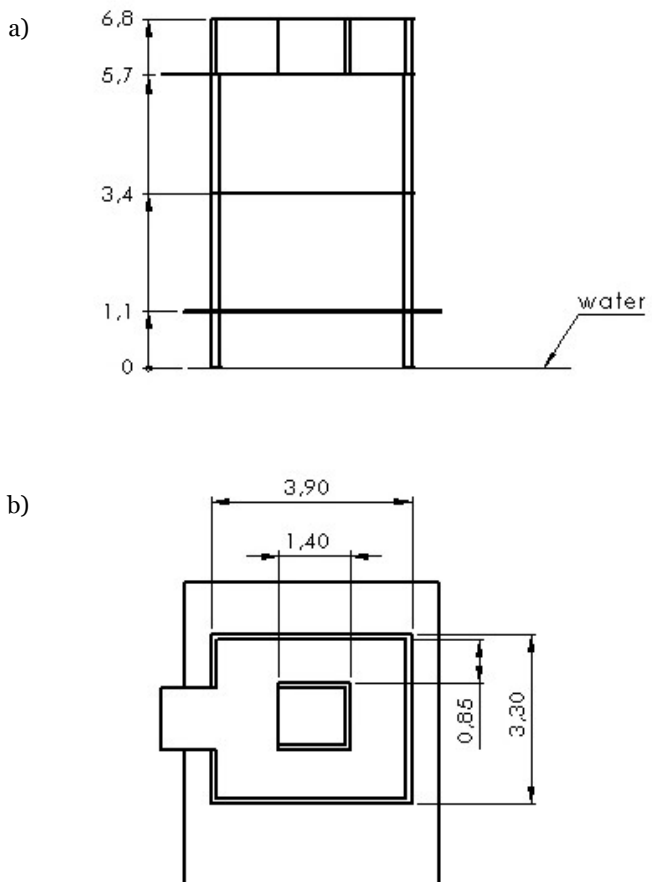

Figure 6: Dimensions of the diving platform in metres, a) – front view, b) – top view.

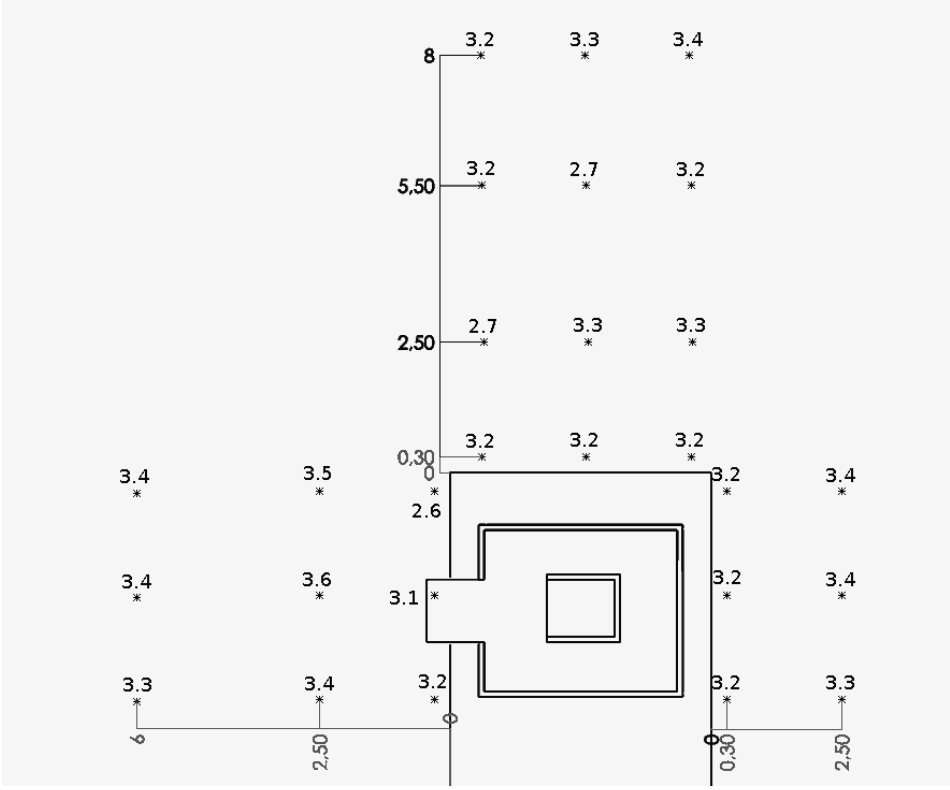

Figure 7: Depth of water around the diving platform of Lake Kääriku. Units are metres.

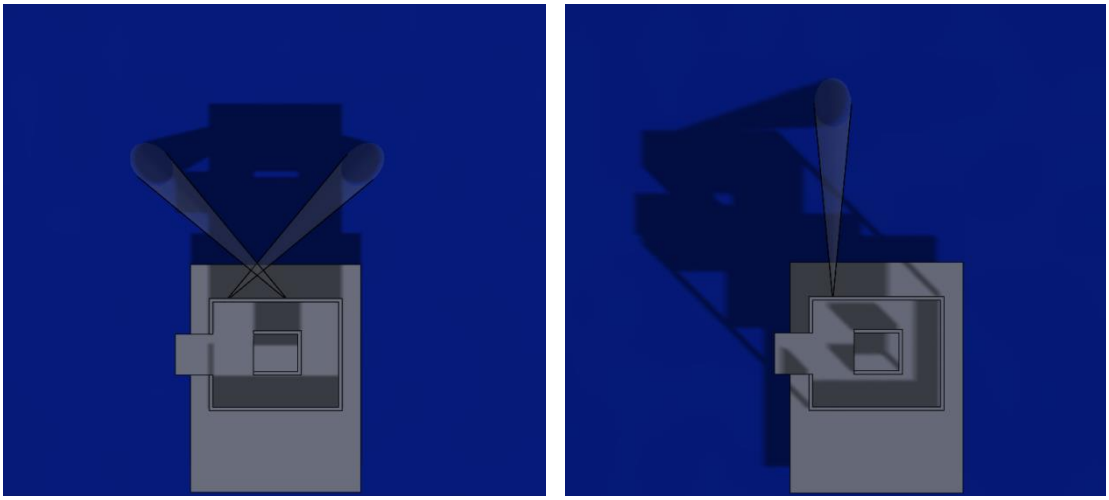

Figure 8: Modelled shadow of the tower around noon (left) and 2 hours before noon (right) in the middle of May. Cones represent the field-of-view of TriOS RAMSES spectroradiometer.

4.3.1 Ancillary data and instruments

Three instruments are available for measuring the volume scattering function (VSF) of water. WET Labs ECO-VSF 3 is a three-angle, three-wavelength volume scattering meter that measures the volume scattering functions at three angles 100°, 125°, and 150° in the backscatter directions and at three wavelengths 470 nm, 532 nm, and 660 nm [4]. WET Labs ECO-BB3 is a three-wavelength backscattering meter [5] that measures the VSF at 124° [6] at three wavelengths 412 nm, 595 nm, and 715 nm. Multi-spectral Volume Scattering Meter (MVSM) is an experimental instrument which can measure VSF with high angular resolution in the range 0.5°...177.5° and up to 10 spectral bands [7].

Spectral absorption and beam attenuation can be measured with WET Labs AC-S with 10 cm path length covering the spectral range (400...730) nm with 4 nm resolution [8].

Chlorophyll a concentration is measured in the laboratory of Limnological Station of the Estonian University of Life Sciences. Water is strained through Whatman GF/F glass microfiber filter with 0.7 µm pore size. Chlorophyll is extracted from the filter with 96% ethanol and the solution is analyzed spectrophotometrically according to ISO 10260:1992 standard. The concentration of chlorophyll a is calculated according to the Lorenzen method [9].

The concentration of total suspended matter (TSM) is measured by straining the carefully mixed water sample through a glass microfiber filter and drying the filter in an oven. The mass of TSM is determined by weighing and concentration is calculated as the ratio of masses of TSM and water sample.

Absorption of coloured dissolved organic matter (CDOM) is measured in (280...800) nm spectral range with Hitachi U-3010 Dual Beam spectrophotometer after straining the sample through a filter with 0.45 µm pore size. Distilled water is used as a reference.

Phytoplankton species composition and phytoplankton biomass is determined using inverted light microscope Ceti Versus, Belgium; magnifications 100× and 400× according to the technique proposed in [10]. At least 400 counting units are counted. The mean volume of each species is measured by approximating the shape of the species to the closest simple geometric form. In case of filamentous forms the length of at least 50 trichomes is measured and the mean length is then used for biomass (wet weight) calculation.

Phytoplankton pigment specific absorption is measured with Hitachi U-3010 Dual Beam spectrophotometer equipped with integrating sphere. Sample is filtrated through GF/F filter and the light transmission of both, pigmented and non-pigmented aquatic particles is measured according to [11]. NaClO is used for bleaching. Chlorophyll-specific absorbance is calculated as a difference between

bleached and non-bleached filter: *aph = atot - adp*, and chl-a specific absorption coefficient is calculated as *aph / (chl a + phaeopigment concentration)*.

Transparency of water can be evaluated with a Secchi disk. There are several variants of Secchi disks, TO uses a ∅20 cm white disk (Figure 9). Secchi disk is lowered into the water until it disappears from view. Attenuation coefficient of water can be estimated from the immersion depth [12].

Figure 9: Secchi disk.

Depth of water can be measured with a Plastimo Echotest 2 handheld depth sounder or with a tape measure. Wind speed is measured with a handheld anemometer АРИ-49. Air and water temperatures are measured with a custom-designed digital thermometer based on a Dallas Semiconductor DS18B20 temperature sensor.

Nikon D5100 digital camera with a Sigma 4.5 mm F2.8 EX DC circular fisheye lens is available for recording cloudiness. The camera can be programmed to time-lapse capture.

AERONET sun photometer Cimel CE318 is located in Tõravere, 30 km north of Lake Kääriku. Atmospheric ozone and water vapour content and aerosol optical depth can be measured on site with Cimel CE-318N-EM-S9 and Microtops II sun photometers.

5 Traceability

Metrological traceability means that an unbroken chain of calibrations is in place for each measurement result relating it with a suitable reference – a primary realization of a respective SI unit - whereby all calibrations of the chain are documented and contribute to the measurement uncertainty. For establishment of the metrological traceability at the TO the reference instruments are calibrated at National Metrology Institutes or accredited calibration laboratories (NPL, UK; MIKES, Finland; Metrosert, Estonia, and TO, Estonia).

5.1 Reference irradiance and radiance sources

The spectral irradiance scale of TO is realized in quartz tungsten halogen (QTH) incandescent lamps. The radiometric standard lamps are of FEL type: 1000 W, quartz-halogen, tungsten double-coiled

filament, operated in the open air with coil in vertical position. The lamps are operated with constant direct current of 8.1000 A or 8.2000 A, depending on the type. The voltage across lamp terminals is approximately (105…110) V. Working time of the lamp after calibration is carefully recorded in order to account for uncertainty increase due to temporal instability of the lamps. Typical ageing rate during a simulated use cycle of a pre-selected, pre-aged modified FEL lamps is described in [13]–[15]. Each lamp has its own alignment jig. The alignment jig is placed in front of the lamp with the grooved surface directed towards the detector. Distance between the lamp and detector is normally 500 mm, and measured with respect to the reference plane defined as the front surface of the lamp socket. Other reference planes like the centre of filament or the surface of the alignment jig are not to be used.

For determination of spectral radiance, the radiation from a calibrated diffuse reflectance plaque is measured. The plaque is illuminated by a calibrated lamp of known spectral irradiance, placed at the distance of at least 500 mm from the plaque. The radiance input optics of the instrument being calibrated is placed at view angle 45° from normal in front of the plaque at a distance of several centimetres, allowing the FOV to be filled by reflected radiation.

5.2 Relation to LCE-1

For LCE-2, link to the SI is provided by the three standard lamps calibrated during LCE-1 at NPL. Traceability of the radiance source used during LCE-2 is also provided by the two calibrated at the NPL radiometers. The radiometric standard lamps of TO have been previously calibrated at the Metrology Research Institute, Aalto University, MIKES. The electrical instruments (multimeters, shunt resistors and current-to-voltage converters) used for operating the lamp and recording the measurement signals are calibrated at national standard of electric quantities, Metrosert ltd. Diffuse reflectance plaque is calibrated in 8°/hemispherical illumination/view configuration at Labsphere Inc. and in 0°/45° configuration during LCE-1 at NPL. Length and distance measurements are traceable to the national standard of length, and temperature measurements to national standard of temperature, Metrosert ltd. Some radiometric, electrical, length and temperature calibrations are done in-house at TO.

5.3 Uncertainty contributions

The uncertainty is calculated from the contributions originating from the spectral irradiance of the standard lamp, including data from the calibration certificate, from interpolation of the spectral irradiance values to the designated wavelengths, from instability of the lamp due to working time elapsed after calibration, from contribution to the spectral irradiance due to setting and measurement of the current of the lamp, from measurement of the distance between the lamp and input aperture of the radiometer, from the spatial uniformity of the irradiance at 500 mm distance, and from reproducibility of the alignment. For the array spectroradiometer uncertainty contributions arising from dark measurements, from repeatability and reproducibility of measurements are included. All uncertainties are given with a coverage factor $k = 2$. In the frame of LCE-2, corrections for linearity, for stray light, for instrument temperature are not applied, and respective uncertainty components are not included.

To minimize the effect of random noise in the measured spectrum, a large number of spectrometer signals are averaged. It is advisable that the number of recorded spectrums in series n and the number of repeated series N were the same for all quantities measured. The same averaging for all signals, and for the ambient background and/or for the instrument's dark responses recorded with different integration times may cause longer recording durations, but it will standardize the Type A estimates and make their combining more reliable.

6 Measurement models

Measurement model is usually a function, which describes the output quantity Y about which information is required as a function f of input quantities X_i which are measured or about which information is available: $Y = f(X_1, X_2, X_3 \ldots)$ [16]. Model function allows also solve the problem of uncertainty propagation from input quantities X_i through f to the output quantity Y if the uncertainties are negligibly small compared with the determined quantity values x_i. In the following paragraphs 6.1 to 6.4 basic models relevant for LCE-2 are described.

6.1 Radiometric sensitivity

6.1.1 Spectral Irradiance Calibrations

For determination of spectral responsivity of the radiometer $R_E(\lambda)$ for the irradiance [17]–[22], it is calibrated against a known source normally placed at the fixed distance from the entrance optics of the radiometer. The lamp-holder and the radiation sensor being calibrated are mounted on the same optical rail but placed in different rooms separated with a bulkhead equipped with a computer-controlled electronic shutter with a ∅64 mm aperture. In order to reduce the effect of stray light two additional baffles (∅60 mm) between the lamp and the radiometer are used. For alignment into the same horizontal optical axis between the lamp and the radiometer a dual beam alignment laser is used. The radiometer being calibrated is mounted on a computer-controlled linear translation stage next to a standard filter radiometer. The positions of both radiometers are carefully adjusted before calibration and saved in the controlling software. This allows fast and accurate swapping of the radiometers. The filter radiometer can be used for monitoring the stability of the standard lamp or for readjustment of the distance between the lamp and sensor if the irradiance level has to be reduced.

As a calibration source the 1 kW FEL lamp is used. The lamp current and voltage are measured by using four-wire sensing, one pair of cables for feeding current to the lamp, and the other to measure the voltage drop on the lamp. The lamp current is measured as the voltage drop on a calibrated shunt resistor. The lamp terminals are connected to a constant current power supply ensuring proper polarity as marked on the lamp. The power supply is turned on and slowly ramped-up to the working current of the lamp. Calibration measurements may be started after at least a 20 min warm-up time. During calibration the voltage across the lamp terminals is also measured, and compared to the voltage measured during the last calibration of the lamp. A significant change in the lamp's operating voltage indicates that it is no longer usable as a reliable working standard of spectral irradiance. On completion of the calibration, the lamp current is slowly ramped down to avoid thermally shocking the filament.

The distance of the lamp is set with the aid of a special length measure made of aluminium alloy. One measurement surface - the lamp socket - is mechanically contacted with one end of the length measure, for the other measurement surface two crossing (120°) laser beams are used, defining so optically the position of the input aperture of detector without mechanical contact. Accuracy of the distance setting is better than 0.2 mm.

If an irradiance sensor at lamp distance of 500 mm is saturated, then in order to reduce the irradiance level the distance between the lamp and sensor should be increased. A new irradiance level $E(\lambda, l)$ can be determined by measuring the optical signal with the aid of standard filter radiometer at the arbitrary filter wavelength as:

$$E(\lambda, l) = E(\lambda, l_0)\frac{F(l) - F_0(l)}{F(l_0) - F_0(l_0)}. \quad (1)$$

Here $E(\lambda, l_0)$ [mW m^{-2} nm^{-1}] is the irradiance from the calibration certificate of the lamp at l_0=500 mm, $F(l)$ is the signal at l and $F_0(l)$ is the respective dark signal.

The raw signal of the radiometer $I(n)$ for the n-th pixel is recorded in digital counts [23]. The total number of pixels (spectral channels), ADC output format and range of gains and integration times are instrument-specific parameters. Wavelength scale of the radiometer given as a function of pixel number n = (1…256) has been provided by manufacturer in the calibration certificate of the radiometer and will not be verified during LCE-2. The respective dark signal $S_{c0}(\lambda)$ is subtracted, and the signal is divided by the spectral irradiance from the certificate of the lamp $E(\lambda, l_0)$ interpolated to the designated wavelength, $\lambda(n)$:

$$R_E(\lambda) = \frac{\left(S_c(\lambda) - S_{c0}(\lambda)\right) C_{\text{stray}} C_{\text{temp}} C_{\text{lin}}}{E(\lambda, l_0)\, G_c}, \quad (2)$$

where G_c is the gain amplification factor of the radiometer, if used at different gains. Correction for the stray light C_{stray} is estimated from a spectral stray light correction matrix of the spectrometer if available; additionally, corrections to account for temperature affecting the instrument responsivity, C_{temp}, and for instrument linearity, C_{lin} have to be estimated, if the instrument is used at different temperatures and/or at different signal levels in calibration and application. For calibration conditions C_{lin} and C_{temp} usually are taken equal to 1.

To derive the irradiance $E(\lambda)$ [mW m^{-2} nm^{-1}] the determined spectral irradiance responsivities $R_E(\lambda)$ have to be applied to subsequent radiometric field measurements $S(\lambda)$ as

$$E(\lambda) = \frac{\big(S(\lambda) - S_0(\lambda)\big) C_{\text{stray}} C_{\text{temp}} C_{\text{lin}}}{R_E(\lambda) G_c}, \tag{3}$$

where $S_0(\lambda)$ are the instrument's dark signal responses determined in the field. In the field measurements (3) the corrections for nonlinearity and for ambient temperature may be much more relevant than in (2).

6.1.2 Spectral Radiance Calibrations

Radiance responsivity calibrations require a uniform Lambertian source of known radiance that will fill the angular field of view (FOV) of the radiance sensor. Most frequently two calibration procedures are used [17], [18]: radiance calibrations by using a reflectance plaque and radiance calibrations by using an integrating sphere.

In the case of first procedure for determination of spectral radiance responsivity of the radiometer, the radiation from a calibrated diffuse reflectance plaque is measured. The plaque is illuminated by a calibrated lamp of known spectral irradiance, placed at the fixed distance of at least 500 mm from the plaque. Baffles with small apertures are placed between the lamp and the diffuser to reduce the stray light. The radiance input optics of the radiometer is placed at view angle 45° from normal in front of the diffuser plaque at a distance of several centimetres, allowing the FOV to be filled by reflected radiation. In this case for calculation of responsivity $R_L(\lambda)$, the reflected radiance $L(\lambda)$ is used instead of spectral irradiance $E(\lambda, l_0)$ from the calibration certificate of the lamp as in expression (1). Reflected radiance $L(\lambda)$ is expressed by:

$$L(\lambda) = \frac{E(\lambda, l_0)}{\pi} R(0°, 45°, \lambda)\,. \tag{4}$$

Here $R(0°, 45°, \lambda)$ is the bidirectional reflectance factor of the diffuser plate taken form the calibration certificate and interpolated to designated wavelength λ.

If a radiance sensor at a lamp distance of 500 mm from the plaque is saturated or in the case of large FOV of the radiance sensor, the distance between the lamp and diffuser should be increased similarly to procedure of equation (1).

In the case of second procedure for calibrating spectral radiance sensors the radiation from a uniformly illuminated integrating sphere is measured. An exit port of the sphere should be large enough to completely fill the sensor's FOV. The target port of the sphere must be large enough to place the sensor so far away that reflections off the sensor's entrance optics will not go significantly back into the sphere. If the sensor is too close, the reflected light can increase the intensity and distort the uniformity of the radiance distribution within the sphere. The spectral radiance scale of an integrating sphere source is determined by comparison with the spectral irradiance scale of a standard lamp.

The spectral irradiance $E(\lambda, d, r_1, r_2)$ of the integrating sphere's exit port is measured using the irradiance scale transfer radiometer. The signal $S(\lambda)$ and respective dark signal $S_0(\lambda)$ are recorded with the source exit port open and covered, and source irradiance $E(\lambda, d, r_1, r_2)$ is calculated using (3).

Assuming a uniform radiance distribution within the sphere's exit port, the spectral radiance scale of the integrating sphere is calculated as

$$L(\lambda) = \frac{E(\lambda, d, r_1, r_2)[d^2 + r_1^2 + r_2^2]}{\pi r_1^2} [1 + \delta + \delta^2 + \cdots]\,, \tag{5}$$

where r_1 is the radius of the circular source aperture, r_2 is the radius of the detector aperture, d is the distance between the apertures, and $\delta = r_1^2 r_2^2 (d^2 + r_1^2 + r_2^2)^{-2}$.

In either approach, the radiance responsivity calibration coefficients $R_L(\lambda)$ of the field radiometer are determined as

$$R_L(\lambda) = \frac{\left(S_{\mathrm{r}}(\lambda) - S_{\mathrm{r0}}(\lambda)\right) C_{\mathrm{stray}} C_{\mathrm{temp}} C_{\mathrm{lin}}}{L(\lambda)\, G_{\mathrm{c}}}, \tag{6}$$

where $S_{\mathrm{r}}(\lambda)$ is the signal measured with the radiance sensor directed to the center of the source aperture, and $S_{\mathrm{r0}}(\lambda)$ is the respective dark signal.

To derive the radiance $L(\lambda)$ [mW m^{-2} nm^{-1} sr^{-1}] the determined spectral radiance responsivities $R_L(\lambda)$ have to be applied to subsequent radiometric field measurements $S_r(\lambda)$ as

$$L(\lambda) = \frac{\left(S_{\mathrm{r}}(\lambda) - S_{\mathrm{r0}}(\lambda)\right) C_{\mathrm{stray}} C_{\mathrm{temp}} C_{\mathrm{lin}}}{R_L(\lambda)\, G_{\mathrm{c}}}. \tag{7}$$

6.2 Tests before radiometric calibrations

6.2.1 Radiance sensor's FOV and response of cosine collectors

Although radiometric calibration coefficients of a radiance sensor do not depend directly on the FOV of the sensor, the FOV must be known for properly setting up the sensor for calibration as the FOV must be uniformly filled during radiometric calibration. In addition, during OC field measurements anisotropic targets such as sky and water are measured and depending on illumination and view configurations the results measured with instruments having different FOV might not be directly comparable.

For determining the FOV of a radiance sensor the device under test is placed on a rotation stage with the rotation axis lying in the plane and crossing the center of the entrance aperture of the radiometer. A stable small light source is placed several metres in front of the radiometer. The FOV is scanned with smaller angular increments in the region of rapid change at the wings of the FOV and larger increments elsewhere resulting in at least 10 measurements inside the FOV and 10 measurements at both wings. The measurements should begin and end with the light source at the optical axis of the radiometer for checking the stability of the source. Alternatively a separate monitor detector can be used for verifying the stability of the lamp.

The entrance optics of an irradiance sensor must provide angular response corresponding to cosine function. Deviation from cosine function can be checked with similar setup as used for measuring the FOV of a radiance sensor. At first the spectrum with the sensor looking straight into the calibration source is recorded. The θ = 0° alignment should place the centre of the cosine collector on the axis of illumination, with the collector surface oriented normal to the axis. For that an alignment laser beam intersecting with the filament of the lamp is aimed at the centre of the collector. The position of the radiometer is adjusted until a mirror held flat against the cosine collector reflects the laser beam back on itself. The rotational scale is zeroed in this position. The laser beam should remain in the centre of the collector when the test instrument is rotated between the angles from 0° to 90°, and the laser beam should just graze the collector's surface at the θ = 90°. In testing directional response of cosine collectors the sensor is rotated in the range 0° to 90° in both rotating directions with ≤5° increments at smaller incidence angles and ≤1° increments at θ > 80°. The accuracy of angle positioning should be at least 0.1°. The measurements are normalized with response of the radiometer at θ = 0°, therefore, measurements at normal incidence should be repeated or a separate monitor detector must be used for the lamp. During the measurements the surface of the cosine collector must be uniformly illuminated.

6.2.2 Polarization sensitivity

Polarization sensitivity of above-water radiance instruments has to be tested before radiometric calibrations, and sensitivity to linear polarization less than 2% is acceptable. The tested radiometer is placed according to the measurement scheme in chapter 6.1.2 on the 45° angle on the calibration table in the rotator mount ensuring that the tested instrument could be freely rotated through 360° around its optical axis. At first radiance data without polarizer are recorded in 2° steps over 360°. Then

immediately in front of the tested radiometer the polarizer is placed, and after alignment the polarized data are recorded with increment of 2° over a full 360° rotation of the tested sensor.

6.2.3 Non-linearity effects

The linearity of the radiometric channels should be determined over the whole range of use if different signal levels in calibration and application are expected.

The values are to be normalized at the gain setting used during absolute calibration that is for the integration time at which the spectrometer was calibrated, see G_c for (2) and (6).

Nonlinearity of gain settings can vary with both wavelength and integration time [24]. Since the spectral power distribution of the test and calibration source may be different, it is advisable to use the test source for the actual nonlinearity measurement of the spectrometer if applicable.

Usually the nonlinearity of the spectrometer gain settings over its spectral range is determined, defined as the relative difference between the actual integration time and that displayed by the spectrometer.

6.2.4 Spectral stray light

When a monochromatic source is measured with a spectrometer, the recorded signal normalized to one is called *spectral line spread function* (LSF) [25], [26]. LSF describes the relative responsivity of each detector array element of the spectrometer to excitation at this particular wavelength. LSFs measured at the central wavelength of every array element of the spectrometer form a *spectral stray light matrix* (SLM). SLM is a square matrix which rows are LSFs, columns of the SLM are *slit-scattering functions* (SSF) [27]. SSF describe the relative spectral responsivities of different spectral bands of the spectrometer. The measured value recorded by a single spectral band is convolution of the optical input signal with the SSF corresponding to that band. When the full SLM of a spectrometer is known, the stray light can be removed from the measured spectrum and the 'true' source spectrum can be restored. This can be done also in the case of the broad-band signals measured from natural objects.

Correction of bandpass and stray light effects can be done by mathematical operation called a spectral deconvolution. Unfortunately, the deconvolution of measured spectra due to noise of the measured signal and/or in the estimated SLM may give unstable results. Therefore, existing correction algorithms of measured spectra often deal with the problem of the stray light or of the bandpass separately, and for getting stable solution different regularisation procedures modifying the SLM are applied. From literature, several deconvolution algorithms can be found, based on either iterative approach [27]–[29] or inverse matrix multiplication proposed by Zong e.a. [19], [23], [25], [26], [30], [31]. A number of techniques dealing only with the bandpass correction are available [32]–[35]. Lately a method for the simultaneous correction of bandpass and stray light effects also has been proposed by Nevas e.a.

At the TO a special study for characterisation of the OCR radiometers for quantification of the effect of stray light and comparison of possible methods for its correction is in progress [2], [3]. In order to apply stray light corrections the individual SLM should be available for each particular spectrometer. Determination of SLM is time consuming and for all instruments participating in comparisons not possible in the time frame of LCE-2.

6.2.5 Ambient temperature

Calibration measurements are usually made in a temperature controlled environment. The array radiometers used for field measurements are used over the temperature range from 2 °C to 35 °C, thus can be affected by various temperature effects, which certainly can increase the measurement uncertainty. Therefore, each instrument must be individually tested and characterized for temperature effects at least in the range from 5 °C to 35 °C. Results are usually presented relative to the instruments response at 20 °C.

Thermal effects can be reliable quantified only in stable conditions. In general, the internal temperature of the tested instrument is lagged behind the ambient temperature. As relaxation after a temperature change depends on the type of spectroradiometer, knowledge of stabilisation time of the particular

instrument is important for successful performance of field measurements. Usually the influence of temperature on the dark signal and responsivity of the radiometer are tested. Ambient temperature can affect also the wavelength positions or cause distortions of the slit function of spectroradiometers restricting the reliable use of instrument for field measurements [36].

Commonly the temperatures cited above are environmental temperatures, but it should be noted that any correction should better use the temperature of the affected element, which is normally inside of the instrument. Thus, the instruments equipped with temperature sensors placed at critical locations within the instrument may be preferable for critical applications. For highest precision, dynamic temperature testing involving temporal transients, as well as possible temperature gradients within an instrument, may be appropriate. For temperature correction the internal temperature of the instrument is preferred to the instantaneous ambient temperature.

6.3 Indoor measurements

Correction for the stray light, C_{stray}, for temperature affecting the instrument responsivity, C_{temp}, and for instrument linearity, C_{lin}, used in the formulas (2), (3), (6) and (7) are calculated according to the specific conditions prevailing during the measurements. As radiometric calibrations are made in a temperature controlled environment and using only one integration time, corrections C_{lin} and C_{temp} are often taken equal to 1. For the field measurements according to (3) and (7), the corrections for nonlinearity and for ambient temperature may be much more relevant. The stray light correction C_{stray}, if available, should be applied to every measured spectrum, not only to the field measurements but also when the standard lamp is measured for the responsivity calibration of the instrument.

6.4 Outdoor measurements

During the primary outdoor exercise [37] [38], [39], the basic quantities subject to comparison will be irradiance and radiance of natural objects (i.e. sky and water surface). Thus, in the case of similar input optics, the indoor measurement equations (3) and (7) will apply. Main differences are related to the greater temporal and spatial variability of the natural objects compared to the laboratory ones (requires better synchronization between the instruments) and the fact that light coming from sky and water surface is partially polarized [40].

In the case of secondary outdoor exrcise, radiometers will be operated in their regular configuration to derive water-leaving radiance L_w [41]:

$$L_w(\lambda) = L_u(\lambda) - \rho(w_s) L_d(\lambda), \tag{8}$$

where
L_u is measured upwelling radiance (including sky glint);
L_d is measured downwelling (sky) radiance;
$\rho(w_s)$ is factor describing surface specular reflection depending on the wind speed w_s [42] :

$$\rho(w_s) = 0.0256 + 0.00039 w_s + 0.000034 w_s^2 \quad \text{for} \quad \frac{L_d(\lambda = 750)}{E_s(\lambda = 750)} < 0.05 \tag{9}$$

and

$$\rho(w_s) = 0.0256 \quad \text{for} \quad \frac{L_d(\lambda = 750)}{E_s(\lambda = 750)} \geq 0.05. \tag{10}$$

Remote sensing reflectance is derived from L_w [38]:

$$R_{RS} = \frac{L_w(\lambda)}{E_d(\lambda)}, \tag{11}$$

where E_d is measured global downwelling (direct + diffuse) irradiance. The measured irradiance and radiance values are handled in the same manner as in 6.3.

Because of different view geometries of instruments and setups participating in the intercomparison, L_w and R_{RS} should be converted to match the nadir viewing angle before comparison as follows [43]–[45]:

$$L_w(\lambda) = L_w(\lambda)\frac{\Re_0}{\Re(\theta', w_s)}\frac{\frac{f_0(\lambda,\tau_a,Chl)}{Q_0(\lambda,\tau_a,Chl)}}{\frac{f(\lambda,\tau_a,Chl,\theta_s,\theta',\Delta\varphi)}{Q(\lambda,\tau_a,Chl,\theta_s,\theta',\Delta\varphi)}}. \quad (12)$$

$\Re(\theta', w_s)$ is geometrical factor accounting for multiple reflections and refractions at the air-water interface, θ' is a refracted view zenith angle

$$\theta' = \arcsin\left(\frac{\sin(\theta_v)}{n}\right), \quad (13)$$

where θ_v is the view zenith angle and n is the refractive index of water. Values of $\Re(\theta', w_s)$ are tabulated in [46] and $\Re_0 = \Re(\theta' = 0, w_s = 0)$.

$f(\lambda,\tau_a,Chl,\theta_s,\theta',\Delta\varphi)$ binds reflectance to the inherent optical properties (IOP) of water and $Q(\lambda,\tau_a,Chl,\theta_s,\theta',\Delta\varphi)$ describes the bidirectional characteristics of the reflectance.

Here $\tau_a(\lambda)$ is the atmospheric aerosol optical thickness;
Chl is chlorophyll *a* concentration;
θ_s is the solar zenith angle;
$\Delta\varphi$ is the relative azimuth angle between solar and viewing directions;
$f_0()$ and $Q_0()$ are normalized values of $f()$ and $Q()$, respectively, i.e. wehre $\theta_s = \theta_v = 0$.

Parameter f/Q is tabulated in [47]. Re-calculation for the particular waterbody might be needed.

7 Measurement instructions

In this chapter, the measurement procedure for both the indoor and outdoor comparison exercises will be described [40]. Considering the SI traceability of remote sensing results, these exercises are logically placed between the laboratory calibration and the actual fieldwork in order to help in detecting and quantifying of the error sources.

The indoor and outdoor comparison exercises follow directly the responsivity calibration of the participating radiometers in the TO-s optical laboratory and the calibration results will be made available to the users.

7.1 Indoor comparison

The indoor intercomparison is meant to be performed by the owner/operator of the radiometer under supervision of the laboratory staff. The light sources, power supplies and monitoring devices are provided by TO and the measurement setup will be prepared considering the stable laboratory conditions. Because of the cleanroom requirements, all instruments brought into laboratory area should be carefully cleaned by the TO-s personnel. It is possible to use TO's computers for instrument control and recording of results to reduce the organizing overhead, assuming that the necessary software is available before the comparison exercise. Internal clocks of the related instruments (including computers) should be synchronized before the measurements.

Two measurement setups will be prepared, one for the responsivity calibration of irradiance sensors according to (2) and other for the responsivity calibration of radiance sensors according to (6). The

calibration setups are established in separate rooms and may be operated simultaneously reducing so the total time needed for all participants to perform the measurements. The measurement geometry will be shown on Fig.xx below. Maintaining the suitable laboratory environment, equipment needed for calibration, monitoring the stability, and alignment of radiometers subject for comparison is provided by the TO's personnel while practical setting up of the radiometer and collecting measurement data in accordance with comparison guidelines is responsibility of the radiometer's operator. A short checklist with all the necessary actions in the right order is provided in comparison guidelines.

7.1.1 Irradiance sensors

For irradiance sensors, a calibrated 1000 W tungsten halogen (FEL) source is used. The lamp setup and monitoring is described in Chapter 4.2.1. The setup of the indoor irradiance comparison is shown in Figure 10.

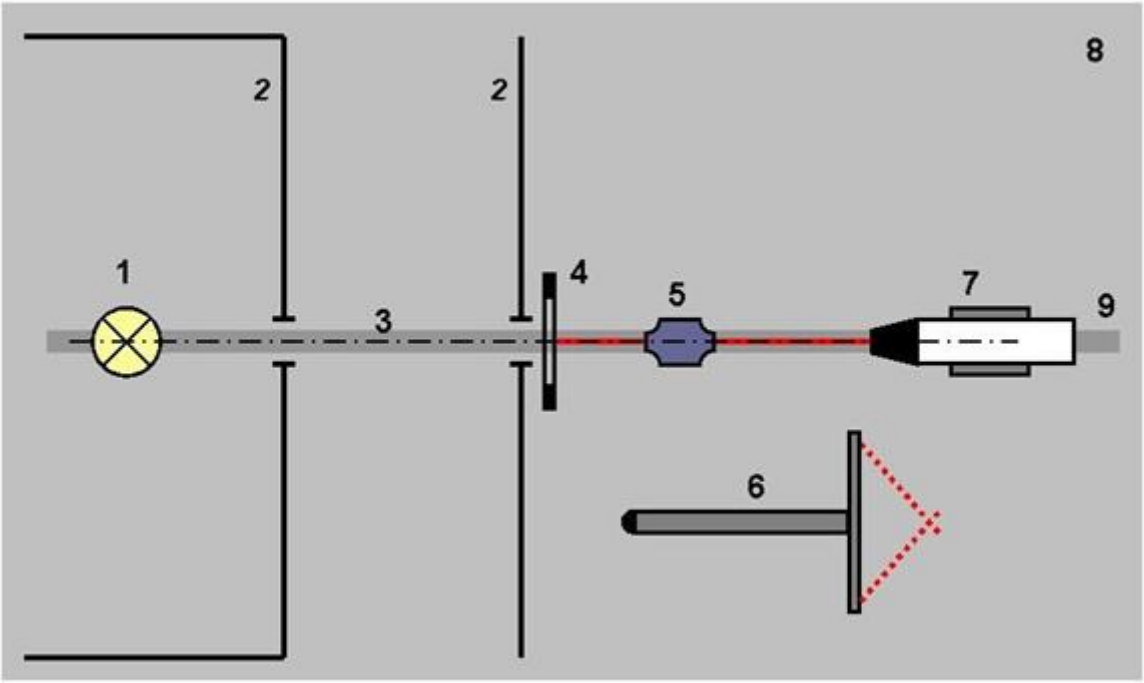

Figure 10: Indoor irradiance comparison. 1 - FEL lamp; 2 - baffles; 3 - main optical axis; 4 - alignment jig; 5 - alignment laser; 6 - distance tool; 7 - radiometer on the support; 8 - optical table; 9 - optical rail.

The irradiance sensor is placed horizontally on the optical axis at the certain distance from the light source, defined by a special target jig. The distance between the lamp and radiometer will be approximately 1 m. The exact value of spectral irradiance is determined by using a standard radiometer according to (1) and corrected by the monitor sensor. The lamp and the target jig are aligned before comparison measurements explicitly by TO's personnel. The participant will have a platform on the optical rail with all the necessary adjustment elements and with a set of clamps to fix the instrument. Participant will adjust the distance between the radiometer and the target jig to be exactly 500 mm by using the special distance tool provided by TO. All cables should be connected to the radiometer before the final alignment.

The user will set up the radiometer as follows:

1) install the temporary dual-beam alignment laser;
2) install radiometer under comparison using any of the supports available;
3) connecting all the necessary cables
4) position the centre of the cosine collector along the laser beam
5) rotate and tilt the radiometer to be parallel to the optical axis

6) set up the distance between alignment jig and radiometer using a special tool
7) repeat steps 4)..6) until no further adjustments are needed.

After the final alignment is approved by the TO's supervisor, the data should be collected as follows:

1) the radiometer readings acquired in series of 30 readings;
2) at least three sets of series separated by no less than one minute interval;
3) the readings should be, whenever possible, taken at three different manually controlled integration times. The longest integration time should be chosen to align the raw signal maximum close (but not exceeding) the saturation level; the other two integration times approximately 2 and 4 times shorter;
4) each recorded value will be equipped with timestamp, integration time and any necessary metadata;
5) recording of the raw data (preferably in human-readable text files) is obligatory; storing of the derived irradiance values is up to the user.

It is possible, within the time frame, to re-align the radiometer for testing the repeatability and rotate the radiometer around its optical axis in order to take into account the properties of the cosine corrector and inherent optical system.

7.1.2 Radiance sensors

For radiance sensors, an integrating sphere with internal quartz tungsten halogen source is used. The sphere source is described in Chapter 4.2.2, equations (4), (5) and (6). Scheme of the setup for the indoor radiance comparison is shown in Fig. 11.

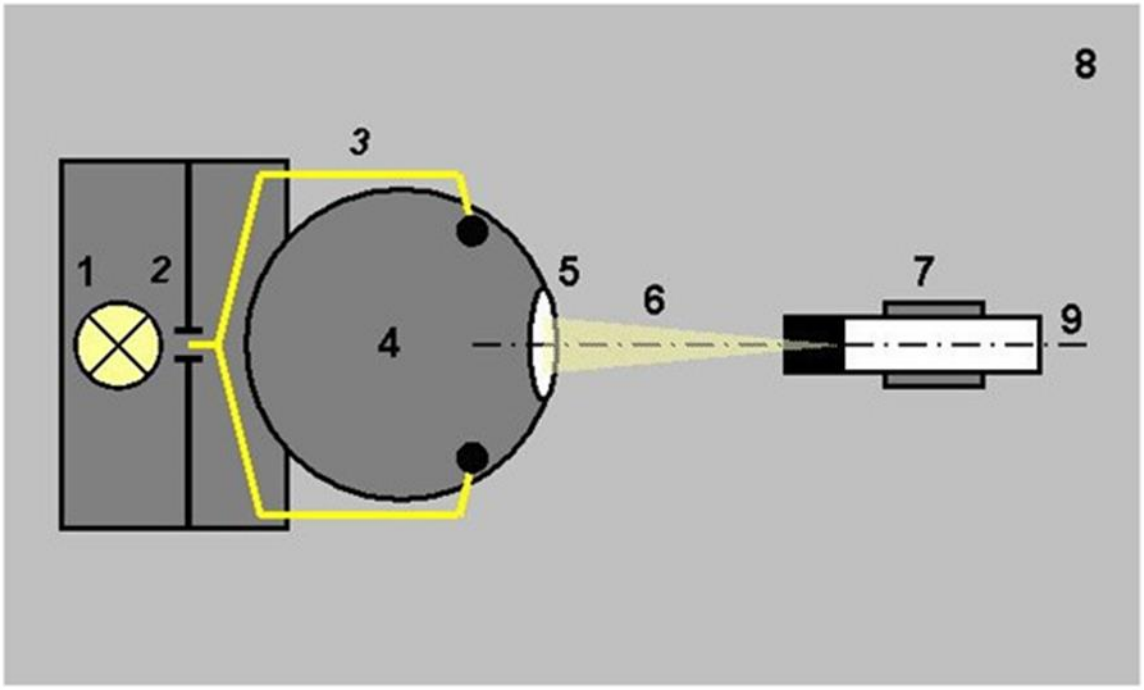

Figure 11: Indoor radiance comparison. 1 - quartz tungsten halogen lamp; 2 - variable slit; 3 - optical fibre; 4 - integrating sphere; 5 - output port; 6 - FOV of the radiometer; 7 - radiometer on the support; 8 - optical table; 9 - main optical axis.

The sphere source is operated explicitly by TO's personnel. The user will be provided with a mechanical platform for mounting the radiometer with all the necessary adjustment elements and a set of clamps to fix the position of the instrument.

The user should align the radiometer along the optical axis crossing the centre of the sphere's output port as follows:

1) the sensor's input window is aligned symmetrically in both the vertical and horizontal directions;
2) distance between the sensor and the sphere is chosen so that the diameter of the output port exceeds the one determined by sensor's FOV by at least factor of two;
3) before the final alignment all cables to the radiometer should be connected;
4) after proper alignment, minor adjustments of the sensor in any direction should not change the raw output signal evidently.

After the final alignment is approved by the TO's supervisor, the data should be collected as described in the previous Chapter. The radiance sensors are operated at two source intensities to simulate the different conditions peculiar to sky and water radiance levels. The source intensity is adjusted by TO's personnel and monitored by a silicon sensor attached to the sphere. It is possible, within the time frame, to re-align the radiometer for testing the experiment's repeatability.

7.2 Outdoor comparison

The main purpose of the outdoor comparison is to establish link between the laboratory and field measurements. Two types of outdoor exercises are planned. Priority is given to the primary comparison where all instruments are pointed to the same physical object and data are acquired synchronously. The instruments in this case will be operated by a single key person while the data is collected by instrument owners/operators. The primary comparison is planned on the first day of the outdoor exercises keeping the second day for spare. During the second step of outdoor comparison, each participant is setting up his/her full measurement setup, pointing to the collectively agreed direction and collecting data during the sparsely defined time frame.

7.2.1 The primary outdoor comparison

In order to eliminate as much as possible the temporal and spatial variability of the natural sources, all radiometers will be tied together to measure approximately the same area of sky or water surface and the data collection will be strictly synchronized. The physical quantities selected for the comparison exercise are absolute spectral irradiance and radiance. The measurement site is described in Chapter 4.3. The radiometers will be set up by TO's personnel based on the information gathered from the users in the earlier phases of this project. The prepared frames will fit all the previously described instruments from the registered participants while last minute changes are not guaranteed. The frame construction will be specified in the final version of this document. The frame will ensure parallelism of optical axes for all the attached radiometers and the absence of shadowing of each other in the case of the irradiance sensors. The manually controlled rotating platform allowing quick change of the sensor azimuth and elevation angles will be provided as well. The radiometers will be operated on the upper platform of the tower.

Responsibility of the participants will be:

1) setting up computers and any necessary devices on the lower platform of the tower;
2) routing and attaching the instrument cables;
3) synchronizing internal clocks of computers and instruments to the UTC;
4) ensuring that all instruments are in operating condition and batteries fully charged;
5) preparing the controlling software for data acquisition with short notification time;
6) preparing logbook for instant measurement data.

Instrument gains and integration times should be selected according to the usual fieldwork practice. Data acquisition is started and finished and the station names announced by the key person operating the instrument frame.

Collecting of the data depends on the weather conditions, but the measurement plan is following:

1) measurement geometry is selected by the key person;
2) station name/number is announced by the key person;
3) station start command is announced by the key person;
4) timestamp is logged and the acquisition of all instruments started by the participants;

5) measurement conditions are constantly logged by all participants;
6) station stop command is announced by the key person;
7) timestamp is logged and the acquisition of all instruments stopped by the participants.

Typical duration of a station will be 30 seconds. The stations can be cancelled afterwards considering the weather/object conditions or technical issues. Environmental parameters, water samples and metadata will be collected by TO's personnel but can be duplicated by the participants if not disturbing the comparison exercise. The measurement sessions will be announced by the key person.

The following terms apply to the data acquisition and are on the responsibility of the participants:

1) each recorded value will be equipped with timestamp, integration time and any necessary metadata;
2) recording of the raw values (preferably in human readable text files) is obligatory; storing of the calculated results is up to the user.

Data processing should follow the guidelines in Chapter 8. Participants will provide both the raw data files and calibrated/filtered/averaged results on per-station basis.

Final analysis of comparison results will be carried out by TO, the supposed primary quantities are [38], [39]:

1) absolute spectral radiance (upwelling and downwelling);
2) downwelling global absolute spectral irradiance;

In order to assess the different FOV-s of the radiance sensors, a derived quantity such as nadir corrected water leaving radiance should be used instead of upwelling and downwelling radiances. Technical details will be discussed in the final version of this document.

7.2.2 The secondary outdoor comparison

During the secondary outdoor comparison, each participant is responsible to set up both the radiometers (using their usual fieldwork configuration) and the logging equipment. The radiometers will be set up on the upper platform of the tower according to the TR8 ("Protocols and Procedures for Field Inter-Comparisons of Fiducial Reference Measurement (FRM) Field Ocean Colour Radiometers (OCR) used for Satellite Validation") of the current project. As an example, the measurement setup with three TriOS RAMSES instruments is shown in Figure 12.

Measurement directions and time frames will be collectively agreed during the exercise while each participant is responsible to collect all the data (when supported by the instruments) needed for comparison of the following physical quantities [38], [39]:

1) water-leaving absolute spectral radiance;
2) downwelling global absolute spectral irradiance;
3) remote sensing reflectance.

Collecting of the weather and metadata (except water samples) is on the participants' responsibility as well.

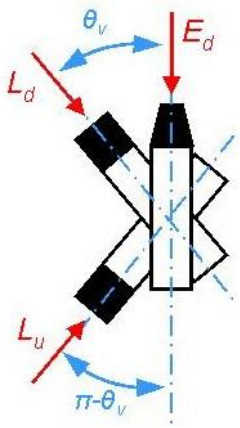

Figure 12 Proposed reflectance measurement setup.

8 Calculations and data processing

The purpose of data processing is to give directions to the users to derive the required quantities, namely absolute spectral irradiance and radiance, using collected raw data, laboratory calibration data and unified algorithms. During all measurements, both in the laboratory and field conditions, the users are encouraged to record the raw instrument data (raw pixel readings, timestamp, signals from the pressure/depth and temperature sensors and so on). Storing the raw data together with the device's calibration history is considered the optimal way to obtain reliable measurement results. In the scope of the comparison exercises, calibration data for all the participating radiometers will be maintained by TO.

8.1 Instrument data processing

The general guidelines for all types of instruments are described here while a detailed example is given in Appendix B. Whenever possible, sensor raw data (e.g. ADC readings) should be stored as the measurement result. If supported by the controlling software, plain text files are preferred.

As in general, these steps in the following order are needed to retrieve irradiance/irradiance values in physical units:

1) subtraction of the dark/background signal
2) linearity correction
3) stray light correction
4) wavelength scale/bandpass correction
5) applying normalized integration time
6) applying radiometric calibration coefficients
7) applying thermal correction coefficients

While not all the corrections are applicable/reasonable for all the instruments, points 1) and 6) are needed as minimum to retrieve the calibrated result. This processing chain should be applied to each raw measurement before any further statistical analysis. As an exception, the outliers are allowed to be removed from the raw dataset before processing if the physical reason can be clearly determined. Based on the corrected and calibrated results, arithmetic average and standard deviation for each series should be calculated.

The following quantities for each series should be calculated by the user and will serve as input for the comparison exercise:

1) start and end time
2) arithmetic mean value

3) standard deviation
4) number of acquisitions
5) number of discarded acquisitions

8.2 Intercomparison

The final analysis of intercomparison results will be carried out by TO. For that, users should provide the collected data - raw data files - and final calibration results, averaged over all valid series recorded, and corrected for significant systematic effects together with relevant uncertainty estimates. The weighted mean of participants would be a preferred reference value [48], [49], if a consistency check by applying a chi-squared test will show a satisfactory agreement between participants. Otherwise the median [50] as largely insensitive to the existence of outliers will be used.

8.3 Data processing example: TriOS RAMSES hyperspectral radiometers

The radiance and irradiance sensors of the TriOS RAMSES family share similar data flow. Each instrument has 256 pixels at fixed wavelengths, about 18 masked pixels to account for the temperature drifts, fixed signal gain, a 16-bit ADC and integration time associated with each spectrum. The integration times can be selected manually or using autoprobe in the range of (4..8192) ms. Each device is equipped with a unique serial number.

Factory or calibration facility provided device files contain following information necessary for raw data processing (see Appendix A):

1) polynomial coefficients binding pixel number to the wavelength;
2) dark_start and dark_stop corresponding to the masked pixels;
3) back1 and back2 for each pixel to restore the dark signal non-uniformity;
4) cal for each pixel, the radiometric responsivity coefficient.

Spectra are recorded in the plain text files (storing into database is implemented as well) containing header with some metadata (instrument's serial number, timestamp, comments, integration time) and columns containing pixel number and ADC raw count. In the first data row (corresponding to the pixel 0), the integration time is coded.

The factory proposed data processing method, covering only the dark signal subtraction and radiometric calibration, is following (see Appendix Bfor numerical example):

1) normalize the raw signal (divide all pixel values by 0x FFFF=65535);
2) subtract from pixel values back1 and scaled with integration time back2;
3) find average value of the painted pixels and subtract from all pixel values;
4) scale all pixel values to 8192 ms and divide by cal to get the calibrated result.

In this simplified schema, thermal effects (except the dark signal drift determined by the masked pixels), non-linearity, bandwidth and stray light are not taken into account, neither is evaluated the measurement uncertainty.

8.4 Uncertainty evaluation

The uncertainty analysis has been carried out according to the ISO Guide to the Expression of Uncertainty in Measurement [16], and to the EA guide EA 4/02. Evaluation is based on the measurement model, which describes the output quantity y as a function f of input quantities x_i: $y = f(x_1, x_2, x_3 \ldots)$. For every input quantity standard uncertainty is evaluated separately. There are two types of standard uncertainties: Type A is of statistical origin; Type B is determined by other means. Both types of uncertainties are indicated as standard deviation, denoted correspondingly by s and u. In calibration of array spectrometers, the uncertainty contributions arising from averaging of a large number of repeatedly measured spectrums is considered as of Type A. Contributions from calibration certificates (lamp, current shunt, multimeter, diffuse reflectance plate etc.), but also from instability and spatial non-uniformity of the lamp are considered of Type B.

9 Reporting of results

Results of the radiometric calibration will be made available by TO to the participants before the indoor comparison exercise. These instant results depend on the instrument type and are, in general, released in the form of device files recognisable by dedicated software that will be used to operate the instruments during the indoor and outdoor comparison exercises. The complete calibration certificates will be released later.

Measurement conditions (environmental, parameters of the waterbody etc.) will be recorded by TO and released to the participants as soon as possible. Example of the station protocol for the outdoor comparison is shown in Appendix.

Collecting, storing, processing and reporting of the instrument data from the indoor and outdoor comparisons is the responsibility of the participants. Both the raw and calibrated/corrected/averaged data should be made available to TO. Calibrated data will be used for the "blind" inercomparison while the raw data is necessary to assess various correction schemes and to detect for possible data processing issues. As a general requirement for the intercomparison, all calibrated/calculated data should include corresponding measurement uncertainties. Guidelines for evaluation of the uncertainties will be given in the final version of this document.

9.1 Indoor comparison

During the indoor comparison, absolute spectral irradiance and radiance of the known stable sources will be measured by the participants under the supervision of TO-s personnel. Averaged values of irradiance/radiance values, standard uncertainties, the start/end times and number of measurements for each series serve as the primary inputs for the intercomparison. TO will provide irradiance/radiance values of the source together with uncertainty estimates for any given measurement series referring to the timestamps, these values will serve as reference values for the indoor comparison. The report template is in Appendix.

9.2 Outdoor comparison

The primary outdoor intercomparison follows the ideology of the indoor comparison and requirements for the reported results are similar. Results of the secondary outdoor comparison will include both the spectral irradiance/radiance values and derived quantities such as L_w, R_{rs}, depending on the measurement geometry. The participants should report all the measured (calibrated) and calculated results together with uncertainties. Detailed report depends on the specific metod and instruments used in the comparison and detailed reporting guidances will be released in the final version of this document. Reference values for the outdoor comparison will be determined as the weighted mean of all specific type results reported by participants, if a consistency check will show a satisfactory agreement. Otherwise the median of all reported results will be used as reference .

10 Conclusions

This information will be provided in the final version of this document.

11 References

[1] G. Zibordi, K. Ruddick, I. Ansko, M. Gerald, S. Kratzer, J. Icely, and A. Reinart, “In situ determination of the remote sensing reflectance: an inter-comparison,” *Ocean Sci.*, vol. 8, pp. 567–586, 2012.

[2] I. Ansko, J. Kuusk, and R. Vendt, “MERIS Validation and Algorithm 4th reprocessing – MERIS Validation Team (MVT),” Tartu Observatory, Tõravere, INTERMEDIATE REPORT No. 1, May 2015.

[3] I. Ansko, J. Kuusk, R. Vendt, and V. Vabson, “MERIS Validation and Algorithm 4th reprocessing – MERIS Validation Team (MVT),” Tartu Observatory, Tõravere, INTERMEDIATE REPORT No. 2, May 2016.

[4] “ECO-VSF 3. Three-angle, Three-wavelength Volume Scattering Function Meter. User’s Guide. Revision M.” WET Labs Inc., 11-Sep-2007.

[5] “ECO 3-Measurement Sensor (Triplet). User’s Guide. Revision M.” WET Labs Inc., 11-Sep-2007.

[6] “Customer Alert: Notice of Clarification of ECO bb angle nomenclature.” WET Labs Inc., 08-Apr-2013.

[7] M. Ligi, A. Reinart, T. Tõnisson, M. E. Lee, E. B. Shibanov, and I. Ansko, "Prototype and first field measurements for Multi-spectral Volume Scattering Meter (MVSM)," in *In proceedings of Measuring and Modeling of Multi-Scale Interactions in the Marine Environment*, Tallinn, Estonia, 2014.
[8] "Spectral Absorption and Attenuation Sensor ac-s. User's Guide. Revision L." WET Labs Inc., 08-Apr-2013.
[9] C. J. Lorenzen, "Determination of Chlorophyll and Pheo-Pigments: Spectrophotometric Equations1," *Limnol. Oceanogr.*, vol. 12, no. 2, pp. 343–346, Apr. 1967.
[10] H. Utermöhl, "Zur Vervollkommnung der quantitativen phytoplankton-methodik," *Mitteilungen Int. Ver. Theor. Angew. Limnol.*, vol. 9, pp. 1–38, 1958.
[11] S. Tassan and G. M. Ferrari, "An alternative approach to absorption measurements of aquatic particles retained on filters," *Limnol. Oceanogr.*, vol. 40, no. 8, pp. 1358–1368, Dec. 1995.
[12] J. E. Tyler, "The secchi disc," *Limnol. Oceanogr.*, vol. 13, no. 1, pp. 1–6, 1968.
[13] N. J. Harrison, E. R. Woolliams, and N. P. Fox, "Evaluation of spectral irradiance transfer standards," *Metrologia*, vol. 37, no. 5, p. 453, 2000.
[14] J. Hartmann, "Advanced comparator method for measuring ultra-small aperture areas," *Meas. Sci. Technol.*, vol. 12, no. 10, p. 1678, 2001.
[15] Y. Ohno and J. K. Jackson, "Characterization of modified FEL quartz-halogen lamps for photometric standards," *Metrologia*, vol. 32, no. 6, p. 693, 1995.
[16] "Guide to the Expression of Uncertainty in Measurement." International Organization for Standardization (ISO), Geneva-1995.
[17] B. Carol Johnson, H. Yoon, J. P. Rice, and A. C. Parr, "Chapter 1.2 - Principles of Optical Radiometry and Measurement Uncertainty," in *Experimental Methods in the Physical Sciences*, vol. 47, C. J. D. and A. C. P. Giuseppe Zibordi, Ed. Academic Press, 2014, pp. 13–67.
[18] S. G. R. Salim, N. P. Fox, W. S. Hartree, E. R. Woolliams, T. Sun, and K. T. V. Grattan, "Stray light correction for diode-array-based spectrometers using a monochromator," *Appl. Opt.*, vol. 50, no. 26, pp. 5130–5138, Sep. 2011.
[19] S. G. R. Salim, E. R. Woolliams, and N. P. Fox, "Calibration of a Photodiode Array Spectrometer Against the Copper Point," *Int. J. Thermophys.*, vol. 35, no. 3–4, pp. 504–515, May 2014.
[20] S. G. R. Salim, N. P. Fox, E. Theocharous, T. Sun, and K. T. V. Grattan, "Temperature and nonlinearity corrections for a photodiode array spectrometer used in the field," *Appl. Opt.*, vol. 50, no. 6, pp. 866–875, Feb. 2011.
[21] L. Ylianttila, R. Visuri, L. Huurto, and K. Jokela, "Evaluation of a Single-monochromator Diode Array Spectroradiometer for Sunbed UV-radiation Measurements¶," *Photochem. Photobiol.*, vol. 81, no. 2, pp. 333–341, Mar. 2005.
[22] G. Seckmeyer, "Instruments to Measure Solar Ultraviolet Radiation Part 4: Array Spectroradiometers (lead author: G. Seckmeyer) (WMO/TD No. 1538). 44 pp. November 2010." WMO, 2010.
[23] M. Talone, G. Zibordi, I. Ansko, A. C. Banks, and J. Kuusk, "Stray light effects in above-water remote-sensing reflectance from hyperspectral radiometers," *Appl. Opt.*, vol. 55, no. 15, pp. 3966–3977, May 2016.
[24] J. L. Mueller, G. S. Fargion, and C. R. McClain, Eds., "Ocean optics protocols for satellite ocean color sensor validation: Instrument specifications, characterization, and calibration." NASA/TM-2003-21621/Rev-Vol II, 2003.
[25] Y. Zong, S. W. Brown, B. C. Johnson, K. R. Lykke, and Y. Ohno, "Simple spectral stray light correction method for array spectroradiometers," *Appl. Opt.*, vol. 45, no. 6, pp. 1111–1119, Feb. 2006.
[26] Y. Zong, S. W. Brown, G. Meister, R. A. Barnes, and K. R. Lykke, "Characterization and correction of stray light in optical instruments," 2007, vol. 6744, p. 67441L–67441L–11.
[27] Kostkowski, *Reliable Spectroradiometry*. Spectroradiometry Consulting, 1997.
[28] S. W. Brown, B. C. Johnson, M. E. Feinholz, Mark A Yarbrough, S. J. Flora, K. R. Lykke, and D. K. Clark, "Stray-light correction algorithm for spectrographs," *Metrologia*, vol. 40, no. 1, p. S81, 2003.
[29] H. Slaper, H. a. J. M. Reinen, M. Blumthaler, M. Huber, and F. Kuik, "Comparing ground-level spectrally resolved solar UV measurements using various instruments: A technique resolving effects of wavelength shift and slit width," *Geophys. Res. Lett.*, vol. 22, no. 20, pp. 2721–2724, Oct. 1995.

[30] M. E. Feinholz, S. J. Flora, M. A. Yarbrough, K. R. Lykke, S. W. Brown, B. C. Johnson, and D. K. Clark, "Stray Light Correction of the Marine Optical System," *J. Atmospheric Ocean. Technol.*, vol. 26, no. 1, pp. 57–73, Jan. 2009.
[31] A. Barlier-Salsi, "Stray light correction on array spectroradiometers for optical radiation risk assessment in the workplace," *J. Radiol. Prot.*, vol. 34, no. 4, p. 915, 2014.
[32] E. I. Stearns and R. E. Stearns, "An example of a method for correcting radiance data for Bandpass error," *Color Res. Appl.*, vol. 13, no. 4, pp. 257–259, Aug. 1988.
[33] Y. Ohno, "A flexible bandpass correction method for spectrometers," in *Proc. AIC Colour 05—10th Congress of the Int. Colour Association*, Grenada, Spain, 2005.
[34] E. R. Woolliams, R. Baribeau, A. Bialek, and M. G. Cox, "Spectrometer bandwidth correction for generalized bandpass functions," *Metrologia*, vol. 48, no. 3, p. 164, 2011.
[35] S. Eichstädt, F. Schmähling, G. Wübbeler, K. Anhalt, L. Bünger, U. Krüger, and C. Elster, "Comparison of the Richardson–Lucy method and a classical approach for spectrometer bandpass correction," *Metrologia*, vol. 50, no. 2, p. 107, 2013.
[36] L. L. A. Price, R. J. Hooke, and M. Khazova, "Effects of ambient temperature on the performance of CCD array spectroradiometers and practical implications for field measurements," *J. Radiol. Prot.*, vol. 34, no. 3, p. 655, 2014.
[37] "MERIS Optical Measurement Protocols Part A: In-situ water reflectance measurements, CO-SCI-ARG-TN-008 Issue 2.0." ESA/ARGANS, Aug-2011.
[38] G. Zibordi and K. J. Voss, "Chapter 3.1 - In situ Optical Radiometry in the Visible and Near Infrared," in *Experimental Methods in the Physical Sciences*, vol. 47, C. J. D. and A. C. P. Giuseppe Zibordi, Ed. Academic Press, 2014, pp. 247–304.
[39] K. G. Ruddick, V. De Cauwer, Y.-J. Park, and G. Moore, "Seaborne measurements of near infrared water-leaving reflectance: The similarity spectrum for turbid waters," *Limnol. Oceanogr.*, vol. 51, no. 2, pp. 1167–1179, Mar. 2006.
[40] N. Fox and M. C. Greening, "A guide to comparisons – organisation, operation and analysis to establish measurement equivalence to underpin the Quality Assurance requirements of GEO, versio-4, QA4EO-QAEO-GEN-DQK-004." GEO, 2010.
[41] J. L. Mueller, C. O. Davis, R. Arnone, R. Frouin, K. L. Carder, Z.-P. Lee, R. G. Steward, S. Hooker, C. D. Mobley, and S. McLean, "Above-Water Radiance and Remote Sensing Reflectance Measurement and Analysis Protocols. In Ocean Optics Protocols For Satellite Ocean Color Sensor Validation, Revision 2." NASA/TM-2000-209966, Aug-2000.
[42] C. D. Mobley, "Estimation of the remote-sensing reflectance from above-surface measurements," *Appl. Opt.*, vol. 38, no. 36, pp. 7442–7455, Dec. 1999.
[43] A. Morel and B. Gentili, "Diffuse reflectance of oceanic waters. II. Bidirectional aspects," *Appl. Opt.*, vol. 32, no. 33, pp. 6864–6879, Nov. 1993.
[44] A. Morel, K. J. Voss, and B. Gentili, "Bidirectional reflectance of oceanic waters: A comparison of modeled and measured upward radiance fields," *J. Geophys. Res. Oceans*, vol. 100, no. C7, pp. 13143–13150, Jul. 1995.
[45] A. Morel and B. Gentili, "Diffuse reflectance of oceanic waters. III. Implication of bidirectionality for the remote-sensing problem," *Appl. Opt.*, vol. 35, no. 24, pp. 4850–4862, Aug. 1996.
[46] "Reference Model for MERIS Level 2 Processing Third MERIS reprocessing: Ocean Branch, PO TN MEL GS 0026 Issue 5." ESA/ARGANS, May-2013.
[47] A. Morel, D. Antoine, and B. Gentili, "Bidirectional reflectance of oceanic waters: accounting for Raman emission and varying particle scattering phase function," *Appl. Opt.*, vol. 41, no. 30, pp. 6289–6306, Oct. 2002.
[48] M. G. Cox, "The evaluation of key comparison data," *Metrologia*, vol. 39, no. 6, p. 589, 2002.
[49] G. Ratel, "Median and weighted median as estimators for the key comparison reference value (KCRV)," *Metrologia*, vol. 43, no. 4, p. S244, 2006.
[50] J. W. Müller, "Possible Advantages of a Robust Evaluation of Comparisons," *J. Res. Natl. Inst. Stand. Technol.*, vol. 105, no. 4, pp. 551–555, 2000.

Appendix A Sample device file of a TriOS RAMSES spectroradiometer

This information will be provided in the final version of this document.

Appendix B Factory proposed data processing method for TriOS RAMSES spectroradiometers

This information will be provided in the final version of this document.